THE EVOLUTION OF ORGANIC MATERIAL FROM ASTEROID 162173 RYUGU. H. G. Changela,[1] Y. Kebukawa,[2] L. Petera,[1] M. Ferus,[1] E. Chatzitheodoridis,[3] L. Nedjl[4] J. Moravcova,[5] P. Krepelka,[5] R. Holbova,[5] J. Novacek,[5] T. Samoril,[6,7] K. Sobotkova,[7] H. Teserova,[7] and D. Zopatok[8] [1]J'Heyrovski Institute of Physical Chemistry, Czech Academy of Sciences, Prague, Czechia. [2]Yokohama National University, Yokohama, Japan. [3]National Technical University of Athens, Greece. [4]Bruno University of Technology, Czechia. [5]Central European Institute of Technology Masaryk University, Brno, Czechia. [6]Central European Institute of Technology Nano, Brno, Czechia. [7]TESCAN ORSAY HOLDING, Brno, Czechia. [8]TESCAN USA Inc, Pennsylvania, USA. Email: changela@unm.edu

Introduction: The *Hayabusa-2* mission successfully returned ~5 g of mm- to cm-sized fragments of Asteroid 162173 Ryugu (Ryugu here on in) for the first time from a carbonaceous asteroid. Two sites were sampled by touch-and-go on the equator of Ryugu, the first from regolith and the second targeted at material ejected from lower depths by a ballistic [1]. Sampling a carbonaceous asteroid provides unique insight into prebiotic evolution in terrestrially unaltered, early Solar System samples from a known planetary body. Ryugu has shown to be of CI (Ivuna-type) composition, lacking any distinct chondrules and calcium aluminum inclusions. It is composed mainly of secondary minerals including phyllosilicate, (Fe, Ni) sulphides, Fe-oxides, carbonates and phosphates [2]. Organic material (OM) is also pervasive, characteristic of OM found in primitive chondrite matrices. Micron to submicron organic particles (OPs) – macromolecular organic objects surrounded by inorganic material – are most abundant, consistent with the morphology and functional chemistry of insoluble organic matter (IOM) [3]. Soluble organic material (SOM) also occurs [4]. This study is on the characterization of a grain from the first touch-and-go site on Ryugu, with a focus on the morphology, distribution and functional chemical variation of OM *in situ* using electron and synchrotron based X-ray microscopy.

Samples & Methods: A0083 (Radegast here on in) is a 1.3 and 1.7 and mm grain from Chamber A of the Hayabusa-2 collector (1st touch-and-go). The grain was prepared and analyzed taking an approach of minimal mechanical damage to the grain for preparation and characterisation. Radesgast was picked up with vacuum tweezers and placed on a clean Au base mounted on an Al stub. An ~2 mm divot was made on the Au for the grain to sit on. An ~1.5 circular hole in clean Al foil was placed over the top of Radegast and fastened at the edge of the stub, exposing the grain out of the hole and securing it. This has the advantage that the grain can be turned over by lifting the foil for any further characterization whilst leaving it in-tact. A grain of Ivuna was also placed on carbon tape on an Al stub and coated with Au, unlike Radegast which remained uncoated for characterisation. *Focused Ion Beam (FIB)* ~100 nm lamella of Radegast were prepared for Scanning Transmission X-ray (STXM) and

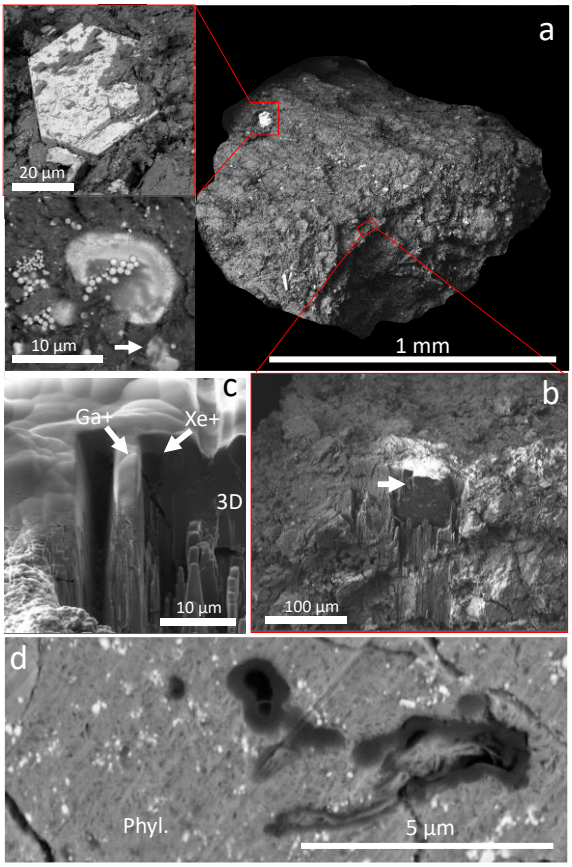

Figure 1. FIB-SEM of A0083. (a) BSE image of A0083 – Radegsat. Inset shows higher magnification of coarse hexagonal Fe sulphide grain (pyrrhotite) and magnetite framboids. Arrowed are also plated Fe-oxide (plaquettes). (b) BSE images Region of 3D tomography from the edge of the grain leading to lamella extraction on left of the 3D volume (arrowed). (c) side view of lamella extractions with Xe+ plasma FIB (*AMBERX*) and Ga+ FIB (*LYRA3*). (d) Higher magnification SE image of organic particles (dark grey) from 1st cross section from the edge of the grain.

Transmission electron Microscopy (TEM). The TESCAN AMBERX and *LYRA3* at TESCAN ORSAY HOLDING and the European Institute of Engineering & Technology (CEITEC)-nano, respectively, were used to compare the effects of Xe+ plasma FIB with Ga+ FIB lamella preparation on the STXM measurements of OM in the samples. In addition, to maximize information from the traditional FIB lamella sample

preparation process, FIB-SEM tomorgraphy was performed from the edge of Radegast (Fig 1b) with the *AMBERX*, at the end of which, the 2 Ga- and Xe- prepared lamella were extracted and thinned down to soft X-ray and electron transparency. An ~60 x 65 x 5 µm volume was sliced and viewed prior to lamella lift-out using TESCAN 3D on the *AMBERX* with sequential 50 nm slices across the volume (Fig. 2). 5 KV EDX maps were made every 5 slices for low KV elemental analysis. Stage rocking was used for cross sectioning the large surface areas.

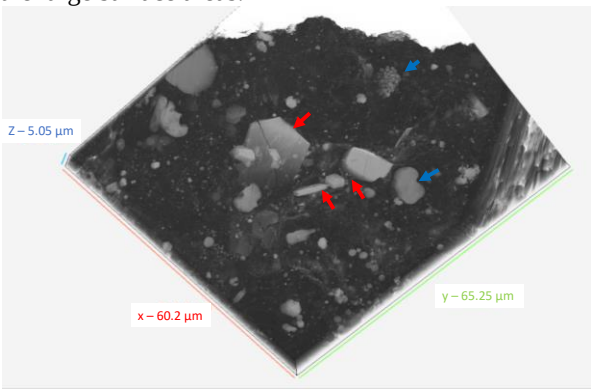

Figure 2. Projection of tomography region prior to lamella extractions at the end of the volume. Red arrows are Hexagonal and plated Fe Sulphides (pyrrhotite). Blue arrows are Fe-oxides. Top blue arrow are magnetite framboids. The entire volume is mostly phyllosilicate (dark grey).

Ultra Microtome Grains of Ivuna were also embedded in molten S for ultramicrotome. 110 nm were prepared using a Leica UC7 at CEITEC-Muni to compare the STXM measurements between Xe-, Ga- FIB lamella and microtome samples. *Scanning Transmission X-ray Microscopy (STXM)* measurements were made at BL 19A at the Photon Factory, Japan. Multiple energy X-ray absorption images from 280 – 320 eV were collected to form stacks, enabling C-K edge X-ray Absorption Near Edge Structure (XANES) spectra to be extracted from any regions of the images.

Results & Discussion: Radegast displays a mineralogy similar to grains from both collection chambers, composed mainly of coarse hexagonal Fe-sulphides (pyrrhotite), widespread Fe-oxides (magnetite framboids) (Fig. 1a), carbonates and phosphates in a phyllosilicate groundmass. This suggests Ryugu's highly altered CI, type 1 composition to be widespread across the asteroid. Micron to submicron OPs are ubiquitous across the tomography cross sections (e.g. Fig.1d). All OPs in the Ga- and Xe-lamella display aromatic/olefinic (C=C)-carbonyl (C=O)-carboxylic/ester (COOH) 3-peak characteristics, similar to OPs identified in the Ivuna microtome sample (Fig. 3). Qualitatively, some particles in Radegast display higher

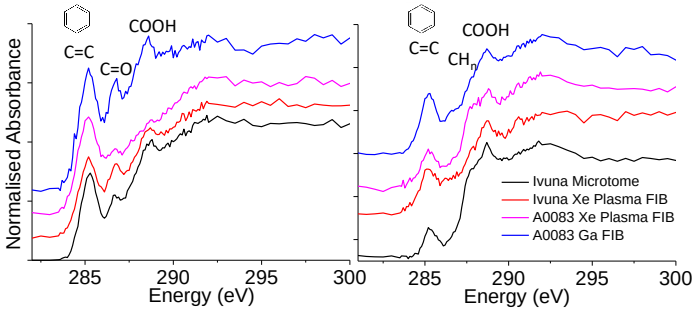

Figure 3. C-XANES of organic particles (left) and phyllosilicate regions - diffuse OM (right).

aromatic/olefinic peak areas in the normalized XANES compared to 3-peak particles in other carbonaceous chondrite matrices (e.g. blue XANES from Ga lamella in Fig 3a). This might reflect higher temperatures of alteration in C1 than the C2/3 petrologic type material. The phyllosilicate regions of Radegast display diffuse OM [5] aromatic poorer and carboxylic richer than the OPs, which was also identified in the Ivuna microtome sample (Fig. 3). [3] identified diffuse OM in a Ryugu grain from the second landing site unique to any OM identified from studies of carbonaceous chondrite matrices *in situ* - an aromatic poor and aliphatic rich fraction, unlike the diffuse OM in Radegast which is characteristic of OM in carbonaceous chondrite hydrated silicates [5]. This could be a preserved organic component from the depths excavated in the second landing site. Further comparison between diffuse OM from both chambers is required to assess this. 3D volume fractions and TEM have yet to be determined of the OPs and secondary minerals. Ryugu should reflect an abundance of OM similar to CI, which is most abundant in chondritic OM such as IOM. Why the most altered chondrites retained a higher abundance of IOM is unclear. Water at one stage present on Ryugu may have transported more IOM. Ice may have accreted either separately or together with IOM leading to the higher abundance in Ryugu/CI. This would imply that IOM was more abundant in the solar nebula where Ryugu accreted its material from than where other primitive chondrite parent bodies accreted from. Alternatively, higher abundances of soluble organic material in solution polymerized more IOM [6], a process on Ryugu which may also preserved the soluble organic content within hydrated silicates.

References: [1] Yada T. et al. (2022) *Nat. Astron.*, 6, 214-220. [2] Nakamura T. et al. (2022) *Science*, abn8671. [3] Ito M. et al (2022) *Nat. Astron.*, 6, 1163-1171. [4] Naroka H. et al. (2022) LPS *XVIII* Abstract #1781 [5] Le Guillou C. et al. *Geochimi. Cosmo. Acta*,131, 368-392. [6] Changela H. G. (2015) *Geochimi. Cosmo. Acta*,159, 285-297.